Chapter 10
Kinetics of Cluster Growth in Fullerene Solutions of Different Polarity

T. V. Tropin, M. V. Avdeev, N. Jargalan, M. O. Kuzmenko and V. L. Aksenov

Abstract Investigations of aggregation and associated kinetic effects, proceeding in various solutions of fullerenes C_{60} present a general interesting subject of research for the last 20–30 years. Since the discovery of fullerene solubility in liquids of different polarity, and also proposition of several methods for their dispersion in water media, these studies are considered particularly interesting from practical point of view. In this chapter we give a brief review of some experimental facts about kinetics of cluster growth in these systems, and present some theoretical models for their description. Most attention is given to such solvents as toluene, benzene and N-methylpyrrolidone (NMP). Some recent ultraviolet-visible (UV-Vis) spectroscopy studies of kinetics of fullerene dissolution, and C_{60}-NMP complexes formation are presented. While in case of low-polar solvents one can easily extract the kinetic constants by applying simple dissolution equations, for the polar solutions the Bouguer-Lambert-Beer law is not applicable and we propose a model for accounting of the complex formation. This allows, again, to extract the dissolution rate constants, and also the complex formation rates. The kinetic theory of cluster formation and growth is based on the nucleation theory. We develop additional suppositions that are required to account for change of fullerene state after interaction with solvents. For obtaining the evolution of the cluster-size distribution function for any stage of cluster growth in the solution, a specific method is applied. Finally, we propose a general model for describing the critical character of fullerenes clusters decomposition in polar solvent on addition of water. This model is based on the specific dependence of molecules solubility in binary mixture on the amount of added water.

T. V. Tropin (✉) · M. V. Avdeev · M. O. Kuzmenko · V. L. Aksenov
Frank Laboratory of Neutron Physics, Joint Institute for Nuclear Research, Joliot-Curie 6, 141980 Dubna, Moscow Reg., Russia
e-mail: ttv@jinr.ru

N. Jargalan
Institute of Physics and Technology, Mongolian Academy of Sciences, Ulaanbaatar, Mongolia

M. O. Kuzmenko
Faculty of Physics, Taras Shevchenko National University of Kyiv, Kyiv, Ukraine

V. L. Aksenov
National Research Centre "Kurchatov Institute", Moscow, Russia

L. A. Bulavin and L. Xu (eds.), *Modern Problems of the Physics of Liquid Systems*, Springer Proceedings in Physics 223,
https://doi.org/10.1007/978-3-030-21755-6_10

10.1 Introduction

The discovery of a new allotropic form of carbon, fullerenes, at the end of the last century [1], is regarded as one of the most important discoveries in the field of nanoscience. The scientific interest to these carbon nanoparticles is supported both by the discovery of new forms of carbon (carbon nanotubes and graphene), and by the prospects for their practical applications [2–5]. Partly, these prospects are related to the fact that fullerenes C_{60}, C_{70} dissolve relatively well in a wide class of organic and inorganic solvents. In solutions, fullerenes exhibit a number of interesting properties [6–8]. These are, for example, solvatochromism and the formation and growth of clusters. As a result of experimental studies of these phenomena, a classification of fullerene solutions according to the type of cluster formation was proposed [3]. The first class consists of non-polar solvents ($\varepsilon < 13$), where fullerenes were initially reported to dissolve in molecular form. The second class is composed of polar fullerene solutions ($\varepsilon \sim 13$–40), while the third one belongs to water and other high-polar liquids. The solutions of the third type are prepared by solvent substitution, or other special procedures required to transfer hydrophobic fullerene molecules to water media [9–12]. Their investigation is an important and regularly revisited subject for different researchers [13–17].

The study and description of the kinetics of formation and growth of clusters in various liquids is important from the point of view of practical applications, and is also an interesting task for applying the theory of cluster formation. Indeed, the character of fullerenes aggregation varies for different classes. For the non-polar solutions, some experimental results contradict one another even at the point of observation of growth of clusters [18–23]. This controversy of opinions regarding cluster formation and growth in low-polar solutions was analyzed in [6, 18] and the conclusion that aggregation is often caused by non-equilibrium conditions was drawn. Some new investigations of C_{60} solution in toluene are reported in [19], with cluster formation attributed to the photoinduced formation of $C_{60}O$ oxides. The dispersion forces between the oxides and fullerenes lead to reversible aggregation effect. These findings are generally in line with our classification [6] and conclusion on non-equilibrium conditions as the reason for cluster formation and growth.

Aggregation in solutions of second type is different: a kinetic transition of fullerene state from molecular to colloidal occurs [24–29]. Many measurements in polar liquids, especially in N-methylpyrrolidone (NMP) [26, 27, 30–32] and pyridine [33, 34] were performed. When modeling the growth of clusters in these solutions, it is necessary to take into account the influence of the formation of fullerene-solvent complexes on the aggregation of C_{60}.

The study and description of the kinetics of formation and growth of clusters in fullerene solutions is important from the point of view of practical applications. The low-polar and polar solutions can be regarded as model systems for studying fullerene aggregation [6, 35, 36], thus opening possibilities for controlling cluster state of C_{60} in water, which is important for perspective application in biomedicine.

Indeed, these systems are also quite interesting for applying the theory of cluster formation [37–40].

In this chapter, we present the results of investigations, both theoretical and experimental, of fullerene solutions in solvents of different polarity. First, a review of experimental investigations for low-polar and polar systems, with accent on our recent ultraviolet-visible spectroscopy (UV-Vis) measurements of kinetics of dissolution and complex formation is given. The second part of the chapter is dedicated to theoretical investigations of kinetics of cluster formation and growth of C_{60} clusters in solutions. A modified approach of the kinetic nucleation theory for describing the evolution of the cluster-size distribution function, $f(r,t)$, is developed. We present results for polar liquids and, finally, a model for mixtures of colloidal fullerene solutions with water is described. A discussion and some conclusions close the paper.

10.2 Experimental Study of Fullerene Aggregation in Solutions

Much research is concentrated on experimental investigations of fullerenes state and behavior in different solutions [6, 30, 41]. Let us briefly review important from our viewpoint findings in the field of clusters formation and growth. As expected, one of the effective and applicable methods here is the dynamic-light scattering (DLS), which was consequently applied for studies of fullerene aggregation in liquids of different polarity [4, 19, 21, 22, 24, 27, 29, 42, 43]. Summarizing, one can say, that in most of these cases, large clusters (size ~100 nm) are observed in such solvents, as benzene [21], toluene [19], pyridine [34], NMP [27, 42, 43], other polar solvents [24, 29] and water [11, 12]. In low-polar and polar solutions one can follow the kinetics of cluster growth [19, 21, 42, 43], it is also possible (in certain cases) to trace cluster decomposition on mechanical agitation of the vial [19, 21]. For the solutions in pyridine and NMP, investigations revealed the effect of cluster destruction on addition of water [33, 44, 45] or low-polar liquid [46, 47]. Finally, in water, fullerene colloidal solutions are very stable [11, 12, 15], this fact being reflected also by ζ-potential of the aggregates.

Big impact and valuable novel information was obtained by using small-angle X-ray and neutron scattering [14, 16, 18, 23, 44, 46, 48]. Method-specific information here is the structure of the clusters. For the case of fullerene-water solutions, for example, it was possible to distinguish one of three proposed shapes of aggregates [15]. For low-polar solutions, indications of two-level structure were reported, and the conclusion on the dense packing in aggregates was also drawn. In most cases, it was concluded, that the density of aggregates is similar to fullerene crystals [15, 44].

Electron microscopy was used for characterization of aggregates in the solution in several works [4, 9, 28, 49]. It must be mentioned, though, that the pre-measurements drying of the sample makes the solution pass through supersaturated state, which may lead to rapid aggregation effects [6, 18]. Thus one can investigate not the natural state

of nanoparticles in the liquid, but the effects occurring in the dried sample. On the other hand, if the clusters were initially formed and stabilized in the solution by certain interactions, the drying may not affect their state and the investigations may be plausible [4, 30].

UV-Vis spectroscopy studies also produce valuable information in this field. The spectrum of C_{60} molecular solution is characterized by an absorption peak at wavelength ~330 nm. Some other peaks at lower λ, and a small peak at ~408 nm may be found. Interactions in the solvent, indeed, affect the basic spectrum, hence new peaks may be detected, or bathochromic/hypsochromic effects observed. The temporal solvatochromic effect observed in solutions of fullerene in NMP or pyridine should be specifically mentioned [33, 50]. If the initial solution is prepared with due care, a characteristic "molecular" spectrum can be measured, yet as time passes the 330 nm peak is gradually smeared, the visual change of the solution color from purple to brown occurs. The final slope is a monotonically decreasing absorption spectrum. The UV-Vis spectrum of C_{60} colloidal solutions in water is similar to the one of a molecular solution, yet the peaks are broader and shifted to higher wavelengths [15, 51].

Recently, an investigation of kinetic processes occurring in fullerene solutions was made using the UV-Vis spectrophotometry method [31, 52]. Considering three solutions, benzene, toluene and NMP, the time evolution of light absorption coefficients was measured at different temperatures and rates of mechanical stirring.

Solubility of fullerene in toluene, benzene and NMP is 2.8 mg/ml, 1.7 mg/ml and 0.9 mg/ml, respectively [8, 53]. The temperature, concentration and dissolution conditions were varied. The equilibrium dissolution conditions and the magnetic stirring at different rates were applied. Measurements of temporal evolution of fullerene concentration in low-polar liquids were based on the Bouguer-Lambert-Beer law, which was applied to the absorption A peak at $\lambda = 408$ nm. An example of measurement results is presented on Fig. 10.1.

To analyze C_{60} dissolution kinetics in [52] the Noyes-Whitney equation was used [54]:

$$\frac{\mathrm{d}x}{\mathrm{d}t} = k(S - x), \tag{10.1}$$

where x is a function of t, reflecting the current solution concentration, S is the saturation concentration or the maximum solution concentration (in case there is no excess fullerene added), k is the dissolution constant. The parameters of (10.1) were determined for more than 10 samples, allowing to analyze their dependencies on preparation conditions [52]. In general, it was reconfirmed, that at equilibrium conditions, fullerene dissolution up to saturation concentration proceeds slowly (~7 days for toluene). On the opposite, in the unsaturated case and especially when stirring is applied, the process is much faster. The characteristic values of dissolution rate parameter k for C_{60} in two liquids are $\sim 2 \cdot 10^{-4}$ s^{-1} for toluene and $\sim 10^{-4}$ s^{-1} for benzene. The applied conditions vary k by an order of magnitude.

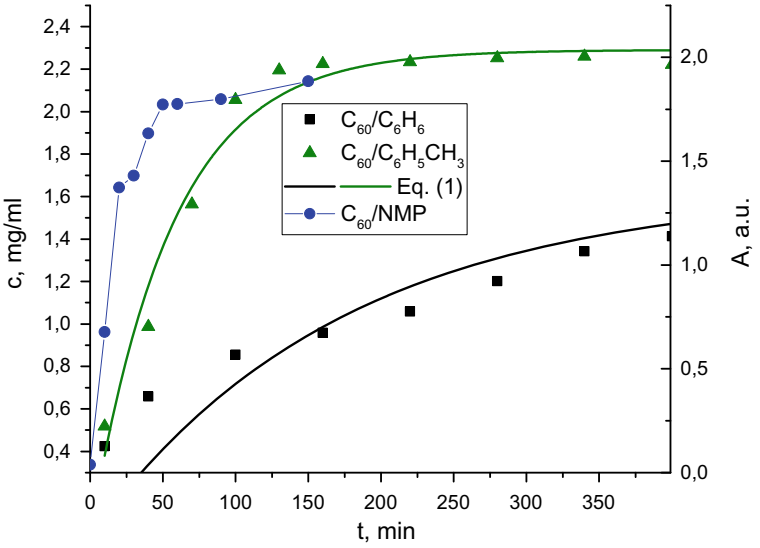

Fig. 10.1 Time evolution of fullerene C_{60} concentration in benzene (black squares) and toluene (green triangles) at different conditions, together with respective change of absorption coefficient A for C_{60}/NMP solution (blue circles) [52]. Bold black and green lines present a fit by dissolution kinetic equation

As it was already discussed, the evolution of the UV-Vis spectrum of the C_{60}/NMP solution is qualitatively different from the case of weakly polar solutions. Temporal solvatochromism is observed for the $A(\lambda,t)$ spectra [26, 30]. There is thus no direct relation between absorption and concentration, because it is affected by the formation of C_{60}-NMP complexes. The investigations of these complexes, occurring in polar C_{60}/NMP solution have been performed, for example, by fluorescence methods [55]. Some DFT calculations [56] also reveal their formation, and another extensive DFT study is underway.

To determine the concentration of the solution at a given point in time from the measured UV-Vis spectrum, we must propose a method for separating the complex formation and cluster growth contributions. In the evolution of the absorption coefficient of light with $\lambda = 330$ nm for a solution of C_{60}/NMP there is a non-monotonic dependence, the output to the equilibrium value occurs at a speed that does not depend on the speed of mixing in a certain range (<300 rpm). The maximum of the absorption coefficient seems to be associated with the disappearance of the characteristic "monomeric" peak and, thus, reflects the relaxation time of one of the processes occurring in the system—the formation of complexes. A rough estimate of this time gives a value of about 3000 s.

To extract the kinetic constants from the measurements, we suppose once again that the dissolution of fullerene is determined by the Noyes-Whitney equation (with the dissolution rate k_1) and that the complexes are formed simultaneously (the reaction rate k_2). Thus, it is possible to introduce a system of kinetic equations [31]:

$$\begin{cases} \frac{dc(t)}{dt} = k_1(C_s - c(t)) \\ \frac{dy(t)}{dt} = k_2(c(t) - y(t)) \end{cases} \tag{10.2}$$

where $c(t)$ is the concentration of "free" fullerene molecules in the solution (those that have not yet formed complexes), $y(t)$ is the concentration of C_{60}–NMP complexes in the system and C_s is the saturation concentration or available concentration of C_{60} (in case the unsaturated solution is prepared). For the considered experiments, when the initial stage is the addition of fullerene to NMP, the initial conditions for (10.18) should be: $c(0) = y(0) = 0$.

After most fullerene molecules form complexes with NMP in solution, the UV-Vis spectrum presents a monotonically decreasing curve. The observed peak at ~330 nm corresponds to the concentration of "free" C_{60} molecules. Thus, this height of the peaks at any time is proportional to $(\varepsilon_1 c(t) - \varepsilon_2 y(t))$, where ε_1 and ε_2 are the absorption coefficients for "free" molecules and complexes, respectively. The values of these coefficients are unknown, we will assume that they are of the same order. This assumption allows us to directly associate the peak height of ~330 nm over the monotonically decreasing type of the UV-Vis spectra with a concentration of "free" C_{60} molecules, equal to $(c(t) - y(t))$. Figure 10.2 shows a typical evolution of the corresponding peak heights for $T = 50$ °C, $v_s = 100$ rpm and $v_s = 400$ rpm. The absorption is normalized to the corresponding concentration of the solution, so it estimates the difference $(c(t) - y(t))$, which can be obtained directly from (10.2):

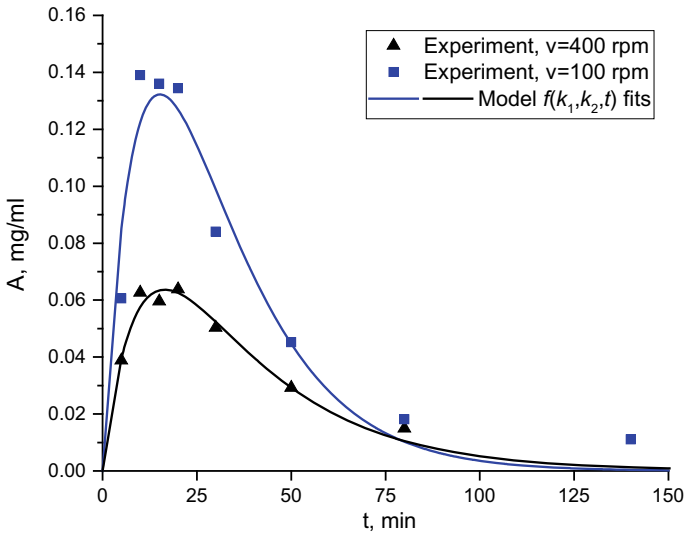

Fig. 10.2 Evolution of normalized peak $\lambda = 330$ nm height above monotonic UV-Vis slope at 50 °C and rotation speeds of 100 rpm (squares) and 400 rpm (triangles). Points represent measured data, lines—fits by using the proposed model [31]

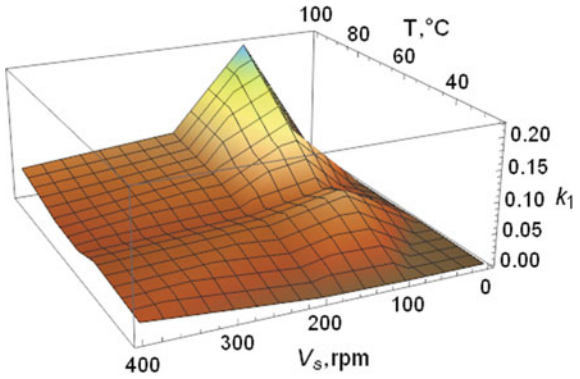

Fig. 10.3 Dependence of kinetic coefficient k_1, in 10^{-4} s^{-1} units, reflecting complex formation speed on solution temperature and stirring rate, obtained from model fitting of UV-Vis data

$$c(t) - y(t) = f(k_1, k_2, t) = \frac{C_s k_1 \left(e^{-k_1 t} - e^{-k_2 t}\right)}{k_2 - k_1} \tag{10.3}$$

The quality of the fit of the experimental data presented in Fig. 10.2 reflects the applicability of the proposed method and approximation. The resulting expression was used to fit various experimental curves to obtain k_1 and k_2 values for different temperatures and mixing rates. An example of the whole obtained 2D dependence of kinetic coefficient on both temperature and stirring rate is presented on Fig. 10.3.

Summarizing, the presented review and results of experimental research of kinetic processes shows, that in low-polar and polar solutions of fullerenes one regularly observes cluster formation and growth. This process is occurring simultaneously with changes of fullerene electronic state after certain interactions with the solvent or oxygen. In the next part of the chapter, we present an approach for theoretical description of kinetics of fullerene aggregation in polar solutions and their mixtures with water.

10.3 Theoretical Description of Kinetics of Fullerene Cluster Growth

10.3.1 C_{60} Aggregation in Polar Solutions

In order to theoretically describe the kinetics of cluster growth in polar (e.g. C_{60}/NMP) solutions, the approach previously developed to describe the nucleation processes and the corresponding segregation of particles during phase transitions is used [57]. The evolution of the cluster size distribution function $f(n,t)$ is obtained from a set of ordinary differential equations. The basic assumptions made to derive the equations are: clusters are quasispherical particles with densities as of a macroscopic solid phase; clusters grow or decompose only by joining and separating one particle (monomer) from the cluster. The second assumption works well for the ini-

tial stages of cluster formation and growth and can be revised for subsequent stages. Nevertheless, we will stay with this approach for the sake of simplicity of the results, thus obtaining a qualitative picture and some general estimates. Consequently, the following system of kinetic equations can be written [40, 57]:

$$\frac{\partial f(n,t)}{\partial t} = w^{(+)}_{n-1,n} f(n-1,t) + w^{(-)}_{n+1,n} f(n+1,t) - w^{(+)}_{n,n+1} f(n,t) - w^{(-)}_{n,n-1} f(n,t), \quad (10.4)$$

where $w^{(\pm)}_{n,m}$ are the probabilities that a monomer is attached/removed from the cluster, thus cluster size changes from n to m per unit time (m is $n+1$ or $n-1$). Hereinafter, the "cluster of size n" is a cluster consisting of n monomers. For comparison with experiments, we will further shift to $f(r,t)$ functions, were r is the cluster radius. The procedure of obtaining $f(r,t)$ from $f(n,t)$ is straightforward. Equation (10.4) with the boundary conditions and the introduction of some modifications will be the basis for calculating the evolution of $f(n,t)$.

From thermodynamic consideration, the ratio of the probabilities of monomer addition and decomposition from the cluster depends on the work of cluster formation, $\Delta G(n)$ [37, 38]:

$$\frac{w^{(+)}_{n-1,n}}{w^{(-)}_{n,n-1}} = \exp\left\{-\frac{\Delta G(n) - \Delta G(n-1)}{k_B T}\right\}. \quad (10.5)$$

In (10.5), $\Delta G(n)$ is the change in the Gibbs free energy of the solution if n monomers form a cluster (work of cluster formation). Thus, if a specific expression is given for $w^{(+)}_{n,n+1}$ and $\Delta G(n)$, then (10.4) are complete.

The expression for the probability of monomer addition is obtained from consideration of the diffusion of monomers from the bulk solution to the cluster surface of size n [57, 58]:

$$w^{(+)}_{n,n+1} = 4\pi D c \left(\frac{3v_s}{4\pi}\right)^{1/3} n^{1/3} \quad (10.6)$$

where D is the diffusion coefficient of the monomers in the solution, c is their concentration, v_s is the volume per particle in the cluster. For a kinetically limited aggregation regime, when the probability $w^{(+)}_{n,n+1}$ is determined by the time of addition of the monomer to the cluster, $w^{(+)}_{n,n+1}$ is proportional to $n^{2/3}$.

In previous works [35, 59, 60] it was shown that the classical liquid drop model is inapplicable for describing cluster growth in fullerene solutions. One of the ways to proceed is to modify the expression for the work of cluster formation $\Delta G(n)$, the so-called limited growth model [61–63]:

$$\Delta G(n) = -n\Delta\mu + \alpha_2 n^{2/3} + k n^{\beta} \quad (10.7)$$

In (10.7), the first two terms correspond to the classical model (the volume and surface terms, respectively). With the third term, as in (10.7), for $k > 0$, $\beta > 1$, cluster growth is limited (the clusters stabilize) at a certain size. This approach, however, requires to physically justify this third term and propose either an estimate or, better, some expressions for k and β values. While this can be done for growth limited by Coulomb interactions, or for nucleation and growth in pores, a straightforward approach for fullerene solutions has not been developed. We will proceed in a different way by modifying the probabilities of cluster growth and decomposition (see below).

The expression for the difference of the chemical potentials of the monomers in the bulk solution and in the cluster, $\Delta\mu$, is taken as for the ideal solution:

$$\Delta\mu = k_B T \ \ln\left(\frac{c}{c_{eq}}\right) \tag{10.8}$$

In (10.18), c is the time-dependent monomer concentration of the segregating phase (single fullerene molecules), and c_{eq} is the equilibrium concentration with respect to aggregation. If the concentration of the solution is higher than c_{eq} (supersaturated solution), then clusters grow. If c is below c_{eq} (unsaturated solution), then the molecular solution is stable. We consider c_{eq} here as an equilibrium concentration with respect to cluster growth. For polar solutions, c_{eq} may be unequal and even much lower than the saturation concentration of the solution, c_{sat}. The reason for this is considered to be interaction between C_{60} and solvent molecules in solution. As experimental studies show, this is a relatively slow kinetic process. Thus, c_{eq} here corresponds to C_{60} complexes with solvent molecules (which tend to aggregate), and c_{sat} corresponds to saturation concentration of unbound fullerene molecules. To some extent, the system under consideration can be compared with solutions of surfactants, where there are also various limiting concentrations, for example, first and second critical micelle concentrations (CMC). The established theory of the kinetics of the growth of micelles is given in [64]. Similarly to the above paper, the numerical approach can be found in [65]. Indeed, in this case, the aggregates in solution are not microcrystallites and qualitatively differ from the solid phase in some properties. Introducing the difference between c_{eq} and c_{sat}, we assume that a similar situation exists for fullerene solutions.

To describe the kinetics of aggregation in polar solutions of fullerenes, it is necessary to propose a modified model that takes into account the effect of the formation of fullerene-solvent complexes on cluster growth. As was shown in [30, 66, 67], the limitation of the processes of growth and decay of clusters due to complex formation can be qualitatively taken into account if the probabilities $w^{(+)}$ and $w^{(-)}$ are changed according to the formula:

$$w'^{(\pm)}_{n,m}(t) = w^{(\pm)}_{n,m}(t) e^{-\frac{t}{\tau}}, \tag{10.9}$$

where τ is the model parameter corresponding to the characteristic time of formation of complexes in the solution and $w'^{(\pm)}_{n,m}(t)$ are the modified probability functions.

Equations (10.4) are solved for a reduced time scale, where the scaling factor is $(4\pi D c_{eq} r_0)$. Further in the text, in most cases, by t we will mean this dimensionless time. In other case, units will be indicated to avoid confusion.

Obtaining a full evolution of $f(n,t)$ using numerical calculations is not possible (for $n \sim 10^8$ and more), so in [68] a method, based on the analytical calculation of the asymptotes of the late stages of cluster growth, developed by Slezov, Lifshitz and Sagalovich [69], is proposed. For the application of this method, it is shown that the distribution functions correspond to analytical functions, obtained by Slezov and colleagues, and the evolution of the average cluster size can be reduced to the $t^{1/3}$ law by transforming the time scale. This allows for any τ to obtain the functions $f(r,t)$ for any value of t. As an example, calculations are made further for the evolution of the cluster state of fullerenes C_{60} in a polar solution.

To simulate the aggregation of fullerene in a particular solvent, it is necessary to set the following system parameters: the surface tension energy, σ, the degree of supersaturation of the initial solution $c(t = 0)/c_{eq}$, the diffusion coefficient of C_{60} in the liquid D, as well as the formation time of the fullerene-solvent complex, τ. For polar solvents (NMP, pyridine, etc.), the values of the first three parameters of the model are unknown. Thus, a "model" solvent will be considered, for which σ is estimated from the calculations of the enthalpy of dissolution of C_{60} in $C_6H_5CH_3$ [70] $(\alpha_2/k_B T = 8)$; the diffusion coefficient is also taken for toluene, $D = 9.1 \cdot 10^{-10}$ m^2/s, the equilibrium concentration is estimated as 10% of the maximum concentration of the solution in NMP, $c_{eq} = 7.525 \cdot 10^{22}$ m^{-3}. An estimate of characteristic time of C_{60}-NMP complex formation was reported in previous section to be $\tau \sim 10^3$ s. The radius of the C_{60} molecule in a solution is $r_0 \sim 0.5$ nm. The transition coefficient for reduced to real time scale is, thus: $4\pi D c_{eq} r_0 \approx 4.3 \cdot 10^5$. It follows that $\tau \approx 4.3 \cdot 10^8$. It is necessary to obtain cluster distribution functions $f(r,t)$ for a given τ. For this, sequential calculations of $f(n,t)$ were performed for a set of τ values in the range from 10^4 to 10^6. This is sufficient to carry out a complete estimate of the evolution of the functions $f(r,t)$.

Analysis of the evolution of the cluster state in a solution we begin with the time dependence of the average particle radius in the solution:

$$\langle r \rangle = \frac{\sum_{n=n_{min}}^{n_{max}} f(n,t) r_0 (n\gamma)^{1/3}}{\sum_{n=n_{min}}^{n_{max}} f(n,t) n}, \tag{10.10}$$

where γ is the packing density of particles in a cluster, n_{max} is the maximum size of particles in the solution, and n_{min}, the minimum size from which the summation starts, is used to eliminate the effect on the <r> value of the equilibrium monomer concentration that is always present in the solution (in present work, $n_{min} = 10$). The calculated dependences <r> for different τ are presented in Fig. 10.4.

As can be seen, the dependence <r> is determined by the value of τ: at times t exceeding τ by two to three times, a stable particle size (and cluster distribution function) in the solution is achieved. In general, the growth of clusters takes place by four stages, the last is the stage of Ostwald ripening, where there is a steady growth

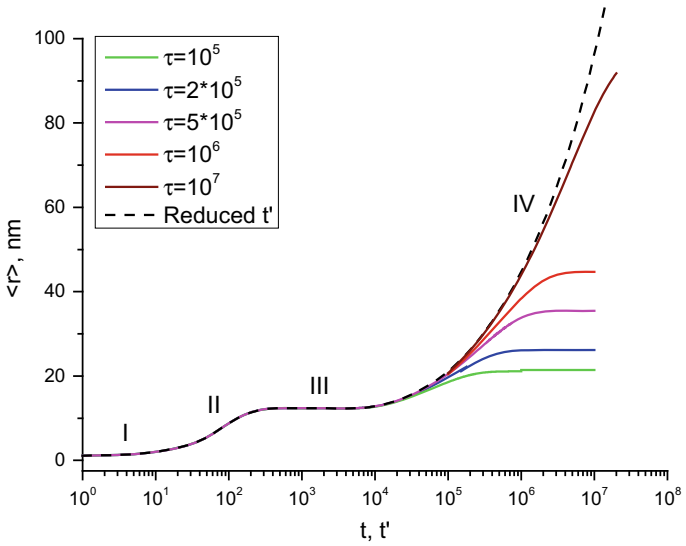

Fig. 10.4 Dependence of the average particle radius, <*r*> in the model solution on time for different values of the model parameter τ (bold curves), and for the case of a reduced time scale t' (dashed curve). Numerals denote different stages of the evolution of the system [68]. The values $\tau = 10^5$, $2 \cdot 10^5$, $5 \cdot 10^5$, 10^6, 10^7 consistently change from the bottom solid curve upwards

of large aggregates. In [71], it was shown that for aggregation limited by diffusion, the so-called "$t^{1/3}$ law" is implemented at this stage:

$$\bar{R}^3 = \bar{R}_0^3 + \frac{4}{9} D\alpha t, \quad \bar{R} >> \bar{R}_0, \tag{10.11}$$

where $\bar{R}_0$ is the average radius of clusters at stage III (independent growth stage). To reduce the dependence of the average particle size to the form (10.11) for a model of limited growth, we need to scale the time with regard to the parameter τ. It can be shown that the t' following expression should be used:

$$t' = \tau\left(1 - e^{-t/\tau}\right). \tag{10.12}$$

In terms of t', all curves <*r*>, regardless of the value of τ, coincide. Moreover, for a sufficiently large time value t', the law (10.11) will be satisfied. Thus, if we take the initial stages of cluster growth (I–III), as well as the transition stage between III and IV from the numerical calculations, then add an expression of the form (10.11), we will have the full dependence of <*r*> on t' at our disposal. For a given τ, the inverse transformation to the time scale t is performed by the formula:

$$t = -\tau \ \ln\left(1 - \frac{t'}{\tau}\right), \quad t' < \tau. \tag{10.13}$$

Similarly, calculations can be performed for the dependence of the number of monomers in a solution, for which an analogue of the "$t^{1/3}$ law" also exists. The monomer concentration in the system is required to calculate the exponentially decaying distribution function of small clusters in size (for $n < n_{\min}$). On Fig. 10.4 the dependency $<r>(t)$, obtained by the described method for $\tau = 10^7$, which roughly corresponds to 10^2 s—the 10% of time of formation of fullerene-NMP complexes in a C_{60}/NMP solution. The dash-dotted line on Fig. 10.4 represents the general dependence of $<r>$ on t' [before applying formula (10.18)]. Calculations for $\tau = 10^8$ are not shown on Fig. 10.4, because in the selected scale $<r>$ almost coincides with the dashed curve.

Since, after the time scale was transformed, the dependence of the basic parameters of the model system is similar to asymptotic calculations for classical kinetic nucleation theory, it can be expected that the cluster size distribution functions coincide with the function proposed in [69]:

$$f(R,t) = n(t)P\left(\frac{R}{\bar{R}}\right)\frac{1}{\bar{R}},$$
$$P(u) = \begin{cases} \frac{3^4 e}{2^{5/3}} \frac{u^2 \exp\left(-\frac{1}{1-(2/3)u}\right)}{(u+3)^{7/3}((3/2)-u)^{11/3}}, & 0 < u < 3/2, \\ 0, & u \geq 3/2 \end{cases} \tag{10.14}$$

where $n(t)$ is the time dependence of the number of particles in the system. For our model system, the cluster size distribution of type (10.14) is already applicable for $t > 2\tau$. Thus performing numerical calculations in the range $t = 0 - 2\tau$ and supplementing them with asymptotic approximations, described by (10.11)–(10.14), we will obtain the whole $f(r,t)$ evolution for a model C_{60} polar solution. The results of such procedure for $\tau = 4 \cdot 10^8$ are presented on Fig. 10.5. Indeed, $f(r,10^9)$ in this case is almost stabilized and will not change much further with time.

The method described here can be utilized for modeling the cluster growth in different polar solutions of fullerenes. A similar approach has been developed in [72] to describe the kinetics of AgCl separation in photochromic glasses already in 1990. In [72] the authors considered Ostwald ripening in a viscoelastic material, obtaining modifications for cluster growth equations with similar exponential decay, as introduced phenomenologically here in (10.9). Moreover, the same changes to the time scale, (10.12), were also considered.

In the next Section, we demonstrate the application of the model results for describing the critical effect of clusters decomposition on dilution of polar fullerene solutions by water.

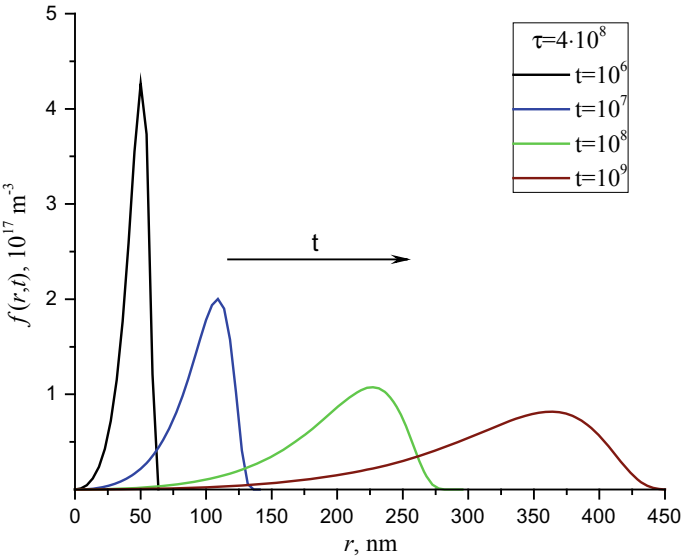

Fig. 10.5 Evolution of size distribution function of fullerene aggregates in a model polar solution, calculated via procedure described in the text and in [68]. The values of model parameters here are: $\alpha_2/k_BT = 8$, $D = 9.1 \cdot 10^{-10}$ m^2/s, $c_{eq} = 7.525 \cdot 10^{22}$ m^{-3}, $\tau = 4 \cdot 10^8$. The corresponding CSDs for $t = 10^7$, 10^8, 10^9 were multiplied by 10, 100 and 500 for better visualizing

10.3.2 Critical Effect of Cluster State Reorganization on Water Addition to C_{60} Polar Solutions

Using neutron scattering, an interesting from the point of view of cluster formation kinetics effect was discovered in [2]. Namely, it was found that when some C_{60} polar solutions are diluted with water, the size of clusters in a solution decreases: from sizes >100 nm to sizes in the range of 10–100 nm. The effect itself is of a threshold nature, and occurs when the volume fraction of added water exceeds ~0.4. The destruction of the clusters occurs immediately after dilution. For a long time, this effect remained unexplained, although this phenomenon seems to be of a general nature (for fullerene solutions, at least).

In [73] it was shown, that direct approach to dilution cannot explain the critical character of the effect. Here we shall recount a specific model of dilution of a colloidal solution with water for a qualitative explanation of this effect [74]. The key factor influencing the change in cluster sizes is the strong dependence of solubility on the composition of the mixture, characteristic of some binary liquids [75, 76]. Estimates of changes in cluster sizes at different stages of growth have been obtained for different volume fractions of added water.

Dilution of the considered colloidal solution with water changes the physico-chemical properties of the solvent, which affects the size distribution of clusters. To reflect this, a dimensionless parameter X, defining the proportion of added water is introduced:

$$X = \frac{V_{H_2O}}{V_{H_2O} + V_{SOL}}, \tag{10.15}$$

where V_{H_2O} is the volume of water added, and V_{SOL} is the volume of the initial solution before dilution. Thus, $X \in [0, 1]$, where 0 and 1 are the limiting values: $X = 0$ corresponds to the case when no water was added to the solution; $X = 1$—infinitely large volume of added water.

The evolution of the system at dilution, qualitatively, is the following. First, at the time of dilution, the values of the function $f(n,t)$ are scaled, since the addition of liquid to the solution changes the concentration of the solute:

$$f'(n, t) = f(n, t)\frac{1 - X}{1 + X}. \tag{10.16}$$

Secondly, the values of the parameters D, c_{eq}, α_2/k_BT and τ change. The ratio of the diffusion coefficients of particles in water and the initial solvent can be estimated by the Stokes-Einstein formula. As a rule, the diffusion coefficient does not change more than twice. Further, we assume that this parameter varies linearly:

$$D' = D_{SOL} + X(D_{H_2O} - D_{SOL}), \tag{10.17}$$

where D' is the value of the diffusion coefficient of the particles in the mixed solvent. The change in τ is not considered in this work; however, upon dilution with water, we restore the original values of the probabilities $\omega^{(+)}$ and $\omega^{(-)}$ [reset the exponent in (10.9)].

The main parameters that determine the behavior of the distribution function after dilution are surface tension (parameter α_2/k_BT) and the equilibrium concentration of c_{eq}. These parameters affect the shape of the potential, which determines the growth and decay of clusters in the solution. The first term in $\Delta G(n)$ changes not only with the cluster size, but also with a change in the concentration of monomers $c(t)$. The value of the α_2 parameter affects the size of the critical cluster in the system. We can approximately suppose that the ratio α_2 in the initial solvent and water is equal to the ratio of the dielectric permittivities of these liquids. In most cases in these calculations, the change in the surface term in $\Delta G(n)$ does not significantly affect the size of large clusters (hundreds of nanometers). We arrive at the conclusion that the main part in describing the effect of cluster decomposition upon dilution is played by the change in the value of c_{eq}.

For a complete formulation of the model, it is necessary to assume the nature of the change in c_{eq} when diluting the initial solvent with water. Fullerene is a hydrophobic molecule; however, its transfer from a polar liquid to water is not equivalent to direct dissolution. For example, in the case of NMP, upon mixing with water, the fullerene-NMP complexes are being transferred (thus, they have non-zero solubility in H_2O). Within the framework of the general model, we assume that the concentration of c_{eq} should continuously change from c_{eq}^{SOL} at $X = 0$ to some unknown value $c_{eq}^{H_2O}$ at $X = 1$. To select the dependence, let us use the results of [75, 76], which describe the use

of NMP as a liquid, which significantly improves the water solubility of drugs. The expression for the concentration that describes this property is:

$$\frac{c_{eq}^{MIX}}{c_{eq}^{SOL}} = \left(\frac{c_{eq}^{H_2O}}{c_{eq}^{SOL}}\right)^{X} \tag{10.18}$$

The value $c_{eq}^{H_2O} < c_{eq}^{SOL}$ is thus a parameter of the model. Further results will be analyzed in sense of a dimensionless parameter $S = c_{eq}^{SOL} \Big/ c_{eq}^{H_2O}$.

The investigation of effects of dilution on $f(n,t)$ via the proposed model was performed for a dimensionally small system, with maximum cluster sizes $n_{max} \sim 10^5$ particles and $\tau = 10^5$. As it was shown in the previous section, all the results can be extrapolated to the real-scale systems.

The dilution in the framework of the proposed approach was modeled for different values of the parameter $c_{eq}^{H_2O}$. In addition to expression (10.18), for the dependence on X, the linear dependence was also checked [74]. It was obtained that only the power-law dependence gives the qualitatively corresponding to the described effect results. For simplicity, t further corresponds to the second stage of the modeling (that is, after dilution) and reflects the elapsed time since the initial solution was diluted.

Figure 10.6 shows the calculated evolution of the average cluster size in a solution in a SOL–H_2O binary mixture for several values of X. Weak dilutions with water do not lead to a change in the cluster state. Starting from a certain, threshold value of X, cluster decomposition upon water addition is observed. For the case shown

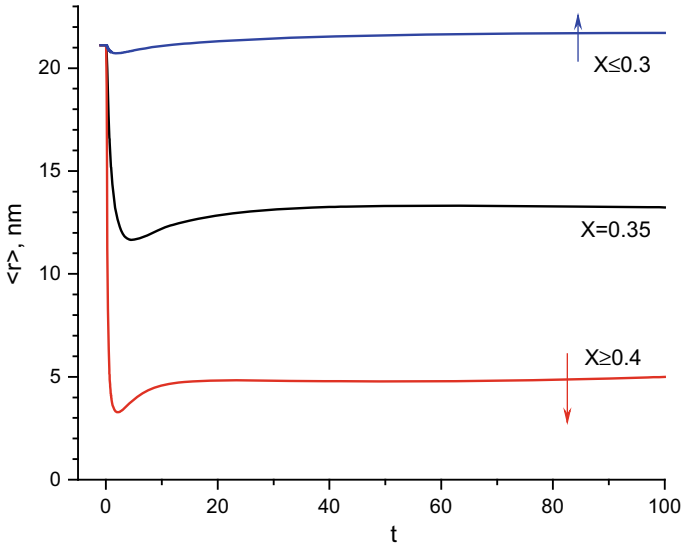

Fig. 10.6 Change of mean cluster size, <*r*>, of fullerenes in binary mixture after water addition to the polar liquid [74]

in Fig. 10.6 this occurs in the region $X_c = 0.35$. It is interesting to note that in the interval $X > 0.4$, the average cluster size drops to a certain value and does not further depend on X. Subsequent slow growth of the clusters is largely determined by the value of D'.

The threshold value X_c, at which cluster decomposition occurs, is determined by the ratio of the saturation concentrations $c_{eq}^{H_2O}$ and c_{eq}^{SOL}. To estimate the nature of this dependence, calculations were performed for different values of S, the results are presented in Fig. 10.7 in the form of the dependence of the average size of aggregates in a solution on X at $t = 1$ after dilution. The position and width of the region in which the transition to the cluster size reduction mode shifts left as S grows.

The cause of the observed in Fig. 10.7 behavior of the integral characteristics of the cluster state is the change of the ratio of the saturation concentration in the solvent mixture and the monomer concentration $f'(n = 1)$. Depending on the S values, there may be a region of X in which a strong supersaturation of the solution $\left(f'(n = 1) \gg c_{eq}^{MIX}\right)$ occurs. Thus, nucleation and growth of clusters rapidly undergoes the initial stages (I–III), which leads to the formation of a new peak in $f'(r,t)$. A bimodal distribution is formed (Fig. 10.8), in which both peaks slowly grow with time. At the same time, as reflected in Fig. 10.7, in this region the average cluster size, <*r*>, decreases in comparison with its value before dilution.

Let us also note, that in the region of large X values there is a threshold X value above which a bimodal distribution is not formed. For example, for $S \sim 10^4$, this

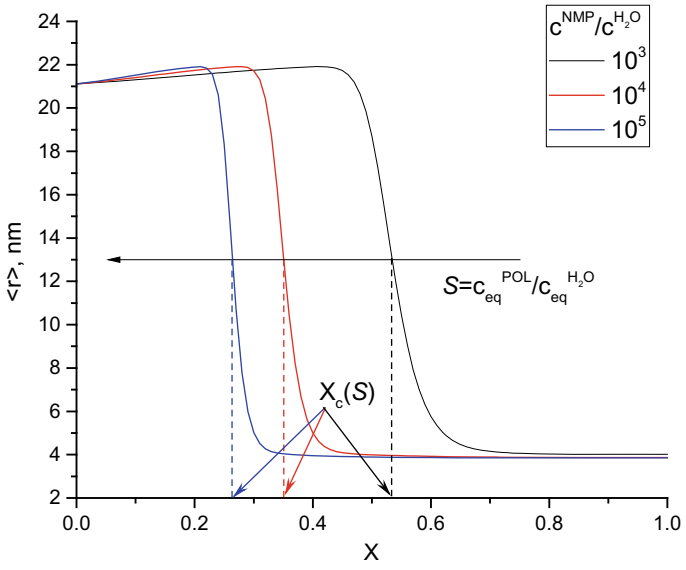

Fig. 10.7 Dependence of the mean cluster size in solution, at moment of time $t = 1$, after dilution by water on the value of X for different values of ratio $S = 10^3$, 10^4, 10^5 (lines from right to left) [74]. The procedure of definition of X_c is visualized

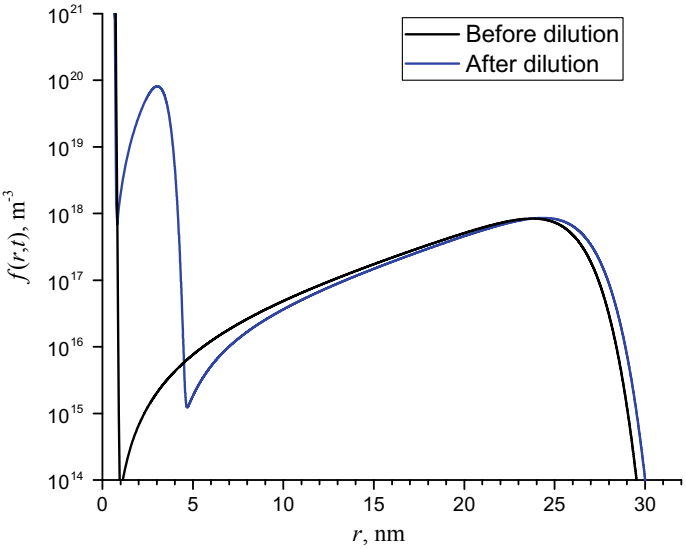

Fig. 10.8 Cluster size distribution functions of initial polar solution of fullerenes (black curve) and for the binary mixture after dilution (blue curve). The $f(r,t)$ after dilution was multiplied by $(1 + X)/(1 - X)$ factor [see (10.16)] for better comparison. Parameters: $S = 10^5$, $X = 0.6$

occurs in the region $X \approx 0.999$–0.9995. At $X > 0.9995$, the dilution transfers the solution to an unsaturated state, so that large clusters will decrease in size, emitting monomer particles into the liquid phase.

Summarizing, a model has been developed for describing the critical character of fullerenes cluster decomposition on water addition to C_{60} polar solution. Moreover, the simulated effect is of a general nature and can be observed in systems in which the stage of Ostwald ripening takes a long time. In these cases, the addition of a solvent to the system, in relation to which the particles are lyophobic, will lead to a significant decrease in the concentration of c_{eq}, and, consequently, the realization of bimodal particle size distributions.

10.4 Discussion

The reviewed investigations of cluster formation and growth, both experimental and theoretical, reveal the following general picture. It is evident that fullerene macromolecules have a tendency to aggregate in the liquids due to several different reasons. These can be solvent-nanoparticle interactions or excitations of fullerene oxidation by light. The size of C_{60} and C_{70} places them at the boundary between colloidal particles and atoms (and small molecules), thus leading to many intriguing effects. The interaction between fullerene molecules in solution occurs via van der Waals forces

(similar to C_{60} crystal) and is generally less or of the order of $k_B T$. Thus aggregation in non-polar liquids will not take place, until fullerene state is changed. In polar liquids lyophobic interactions may shift the state towards cluster growth, yet one can argue that if the equilibrium dissolution to molecular state is observed for some systems, then aggregation without additional effects is against the second law of thermodynamics. Thus most probably in these cases the aggregation also occurs via dispersion forces between fullerene-solvent complexes. The colloidal water solutions of fullerenes in this sense are standing separately, because they require either very intense treatment or transfer of already aggregated particles into water. A number of density-functional theory simulations is being performed presently, to enlighten additionally interactions of fullerenes in different media.

The developed theoretical models aim at describing the kinetics of fullerene aggregation from a general viewpoint. While initial attempts of considering low-polar solutions were made [36, 77], the obtained results are mostly applicable to polar C_{60}/NMP and similar systems. To some extent this is due to the basis of the theory on cluster formation and growth by nucleation in the liquid media [78]. We thus suppose the existence of a kinetic barrier, and also must define the value of c_{eq} as the equilibrium concentration of monomers with solid phase at a planar interface. For low-polar solutions, generally $c_{eq} \approx c_{sat}$, and thus aggregation via nucleation will proceed only if some non-equilibrium methods will be utilized to obtain the supersaturated solutions. For $c_{eq} \sim 2c_{sat}$, for example, the cluster growth will be quite limited in low-polar C_{60} solutions. On the other hand, one can imagine $c_{eq} \ll c_{sat}$ in polar solutions, where c_{eq} now corresponds to solubility of fullerene complexes with NMP. The additional models of confined growth were proposed for accounting of this effect.

On the other hand, a perspective for description of kinetics of fullerene aggregation in such solvents, as toluene and benzene, must be, from our viewpoint, based on applying segregation equations exploiting the hypothesis of binding of fullerene oxides with each other and C_{60} molecules in these media. For these types of modeling, a set of kinetic equations for two-dimensional cluster size distribution functions must be developed and solved numerically. This work is being performed at present.

Further, the developed method for obtaining cluster-size distribution functions for any stage of aggregation in the solution can be applied, for example, for modeling the small-angle scattering curves [71], or for comparison of the results with DLS measurements, which have been performed quite some time ago [28, 42] or recently [19], and are also underway for these and other liquids. The application of these models allows also to investigate such effects as dissolution by water [73, 74]. It is also possible to generalize the developed model of dissolution to account for addition of any other liquid to the system. Three different situations must be considered in this case: the addition of a low-polar liquid to the solution, $\varepsilon_{LIQ} < \varepsilon_{POL}$, addition of similar or the same liquid to the system, $\varepsilon_{LIQ} \sim \varepsilon_{POL}$, and, finally, addition of a high-polar liquid, with $\varepsilon_{LIQ} > \varepsilon_{POL}$. Thus we have to consequently consider a dissolution of polar liquid by each of three types of fullerene solutions, as proposed by the classification in [6]. In this work and in [74] we have considered only the third case, basing, moreover, on the experimental observation for water only [44].

Let us mention, that there exist several works, where similar effects were revealed and investigated for other types of relation between ε_{LIQ} and ε_{POL} [46, 47, 79]. The consideration of these effects and development of a generalized model of dissolution is an interesting research problem.

10.5 Conclusions

The present chapter consists of a review of investigations of fullerenes cluster growth in different solutions. The experimental investigations of these systems are based on a number of different methods, such as dynamic-light scattering, UV-Vis spectrophotometry, electron microscopy, small-angle neutron and X-ray scattering and others. A general classification of fullerene solutions with respect to cluster formation and growth properties can be given, revealing three distinctive classes of systems. We present the measurements of kinetic constants, namely the dissolution rate for low-polar systems at different temperatures and conditions. Additionally, a model-based UV-Vis investigation of kinetics of both dissolution and complex formation is reported, allowing to obtain both constants for these processes.

The theoretical description is based on the kinetic nucleation theory, with confined growth introduced additionally. Thus, the set of kinetic equations is modified to account for complexes formation and segregation in the solution. We have developed a method for obtaining the cluster-size distribution functions, $f(r,t)$ at any stage of systems evolution. The results of its application are used elsewhere, for example, to model the dependence of SANS curves on time of measurement. Here, on the other hand, we review the model of addition of water to polar C_{60} solution, which is developed for description of the critical character of the cluster state decomposition. In the final part of the paper we discuss the obtained results, reveal and propose further perspectives for developments in the field of investigation.

Acknowledgements This research is supported by RBFR (project no. 17-52-44024 Mong_a).

References

1. H.W. Kroto, J.R. Heath, S.C. O'Brien, R.F. Curl, R.E. Smalley, C_{60}: Buckminsterfullerene. Nature **318**, 162–163 (1985). https://doi.org/10.1038/318162a0
2. S. Bosi, T. Da Ros, G. Spalluto, M. Prato, Fullerene derivatives: an attractive tool for biological applications. Eur. J. Med. Chem. **38**, 913–923 (2003). https://doi.org/10.1016/j.ejmech.2003.09.005
3. B.C. Thompson, J.M.J. Fréchet, Polymer-fullerene composite solar cells. Angew. Chemie Int. Ed. **47**, 58–77 (2008). https://doi.org/10.1002/anie.200702506
4. L.A. Bulavin, Y. Prylutskyy, O. Kyzyma, M. Evstigneev, U. Ritter, P. Scharff, Self-organization of pristine C_{60} fullerene and its complexes with chemotherapy drugs in aqueous solution as promising anticancer agents (2018), pp. 3–22. https://doi.org/10.1007/978-3-319-61109-9_1

5. R. Bakry, R.M. Vallant, M. Najam-ul-Haq, M. Rainer, Z. Szabo, C.W. Huck, G.K. Bonn, Medicinal applications of fullerenes. Int. J. Nanomed. **2**, 639–649 (2007). http://www.pubmedcentral.nih.gov/articlerender.fcgi?artid=2676811&tool=pmcentrez&rendertype=abstract
6. M.V. Avdeev, V.L. Aksenov, T.V. Tropin, Models of cluster formation in solutions of fullerenes. Russ. J. Phys. Chem. A **84**, 1273–1283 (2010). https://doi.org/10.1134/S0036024410080017
7. V.N. Bezmel'nitsyn, A.V. Eletskii, M.V. Okun', Fullerenes in solutions, Uspekhi Fiz. Nauk. 168, 1195 (1998). https://doi.org/10.3367/ufnr.0168.199811b.1195
8. Y. Marcus, A.L. Smith, M.V. Korobov, A.L. Mirakyan, N.V. Avramenko, E.B. Stukalin, Solubility of C 60 fullerene. J. Phys. Chem. B. **105**, 2499–2506 (2001). https://doi.org/10.1021/jp0023720
9. G. Andrievsky, V. Klochkov, E. Karyakina, N. Mchedlov-Petrossyan, Studies of aqueous colloidal solutions of fullerene C_{60} by electron microscopy. Chem. Phys. Lett. **300**, 392–396 (1999). https://doi.org/10.1016/S0009-2614(98)01393-1
10. J.A. Brant, J. Labille, J.-Y. Bottero, M.R. Wiesner, Characterizing the impact of preparation method on fullerene cluster structure and chemistry. Langmuir **22**, 3878–3885 (2006). https://doi.org/10.1021/la053293o
11. S. Andreev, D. Purgina, E. Bashkatova, A. Garshev, A. Maerle, I. Andreev, N. Osipova, N. Shershakova, M. Khaitov, Study of fullerene aqueous dispersion prepared by novel dialysis method: simple way to fullerene aqueous solution, fullerenes. Nanotub. Carbon Nanostruct. **23**, 792–800 (2015). https://doi.org/10.1080/1536383X.2014.998758
12. M.E. Hilburn, B.S. Murdianti, R.D. Maples, J.S. Williams, J.T. Damron, S.I. Kuriyavar, K.D. Ausman, Synthesizing aqueous fullerene colloidal suspensions by new solvent-exchange methods. Colloids Surf A Physicochem. Eng. Asp. **401**, 48–53 (2012). https://doi.org/10.1016/j.colsurfa.2012.03.010
13. Y.I. Prylutskyy, V.I. Petrenko, O.I. Ivankov, O.A. Kyzyma, L.A. Bulavin, O.O. Litsis, M.P. Evstigneev, V.V Cherepanov, A G. Naumovets, U. Ritter, On the origin of C_{60} fullerene solubility in aqueous solution. Langmuir **30**, 3967–3970 (2014). https://doi.org/10.1021/la404976k
14. P. Scharff, K. Risch, L. Carta-Abelmann, I.M. Dmytruk, M.M. Bilyi, O.A. Golub, A.V. Khavryuchenko, E.V. Buzaneva, V.L. Aksenov, M.V. Avdeev, Y.I. Prylutskyy, S.S. Durov, Structure of C_{60} fullerene in water: spectroscopic data. Carbon N. Y. **42**, 1203–1206 (2004). https://doi.org/10.1016/j.carbon.2003.12.053
15. M.V. Avdeev, A.A. Khokhryakov, T.V. Tropin, G.V. Andrievsky, V.K. Klochkov, L.I. Derevyanchenko, L. Rosta, V.M. Garamus, V.B. Priezzhev, M.V. Korobov, V.L. Aksenov, Structural features of molecular-colloidal solutions of C_{60} fullerenes in water by small-angle neutron scattering. Langmuir **20**, 4363–4368 (2004). http://www.ncbi.nlm.nih.gov/pubmed/15969139
16. A.A. Khokhryakov, M.V. Avdeev, T.V. Tropin, G.V. Andrievskiĭ, L.A. Bulavin, Y.A. Osip'yan, V.L. Aksenov, Small-angle neutron scattering by colloidal solutions of fullerene C_{60} in water, Crystallogr. Reports **49**, S142–S147 (2004)
17. A.O. Khokhryakov, M.V. Avdeev, V.L. Aksenov, L.A. Bulavin, Structural organization of colloidal solution of fullerene C_{60} in water by data of small angle neutron scattering. J. Mol. Liq. **127**, 73–78 (2006). https://doi.org/10.1016/j.molliq.2006.03.019
18. M.V. Avdeev, T.V. Tropin, I.A. Bodnarchuk, S.P. Yaradaikin, L. Rosta, V.L. Aksenov, L.A. Bulavin, On structural features of fullerene C_{60} dissolved in carbon disulfide: complementary study by small-angle neutron scattering and molecular dynamic simulations. J. Chem. Phys. **132**, 164515 (2010). https://doi.org/10.1063/1.3415500
19. R. Dattani, K.F. Gibson, S. Few, A.J. Borg, P.A. DiMaggio, J. Nelson, S.G. Kazarian, J.T. Cabral, Fullerene oxidation and clustering in solution induced by light. J. Colloid Interface Sci. **446**, 24–30 (2015). https://doi.org/10.1016/j.jcis.2015.01.005
20. T. Tomiyama, S. Uchiyama, H. Shinohara, Solubility and partial specific volumes of C_{60} and C70. Chem. Phys. Lett. **264**, 143–148 (1997). https://doi.org/10.1016/S0009-2614(96)01290-0
21. Q. Ying, J. Marecek, B. Chu, Slow aggregation of buckminsterfullerene (C_{60}) in benzene solution. Chem. Phys. Lett. **219**, 214–218 (1994). https://doi.org/10.1016/0009-2614(94)87047-0

22. N.O. Mchedlov-Petrossyan, Fullerenes in molecular liquids. Solutions in "good" solvents: another view, J. Mol. Liq. **161**, 1–12 (2011). https://doi.org/10.1016/j.molliq.2011.04.001
23. G. Török, V.T. Lebedev, L. Cser, Small-angle neutron-scattering study of anomalous C_{60} clusterization in toluene. Phys. Solid State **44**, 572–573 (2002). https://doi.org/10.1134/1.1462711
24. S. Nath, H. Pal, A.V. Sapre, Effect of solvent polarity on the aggregation of C_{60}. Chem. Phys. Lett. **327**, 143–148 (2000). https://doi.org/10.1016/S0009-2614(00)00863-0
25. S. Nath, H. Pal, A.V. Sapre, Effect of solvent polarity on the aggregation of fullerenes: a comparison between C_{60} and C_{70}. Chem. Phys. Lett. **360**, 422–428 (2002). https://doi.org/10.1016/S0009-2614(02)00780-7
26. O.A. Kyzyma, M.V. Korobov, M.V. Avdeev, V.M. Garamus, V.I. Petrenko, V.L. Aksenov, L.A. Bulavin, Solvatochromism and fullerene cluster formation in C_{60}/N-methyl-2-pyrrolidone. Fuller. Nanotub. Carbon Nanostruct. **18**, 458–461 (2010). https://doi.org/10.1080/1536383x.2010.487778
27. N.P. Yevlampieva, Y.F. Biryulin, E.Y. Melenevskaja, V.N. Zgonnik, E.I. Rjumtsev, Aggregation of fullerene C_{60} in N-methylpyrrolidone. Colloids Surf. A Physicochem. Eng. Asp. **209**, 167–171 (2002). https://doi.org/10.1016/S0927-7757(02)00177-2
28. R.G. Alargova, S. Deguchi, K. Tsujii, Stable colloidal dispersions of fullerenes in polar organic solvents. J. Am. Chem. Soc. **123**, 10460–10467 (2001). http://www.ncbi.nlm.nih.gov/pubmed/11673976
29. N.O. Mchedlov-Petrossyan, N.N. Kamneva, Y.T.M. Al-Shuuchi, A.I. Marynin, O.S. Zozulia, Formation and ageing of the fullerene C_{60} colloids in polar organic solvents. J. Mol. Liq. **235**, 98–103 (2017). https://doi.org/10.1016/j.molliq.2016.10.113
30. T.V. Tropin, N. Jargalan, M.V. Avdeev, O.A. Kyzyma, R.A. Eremin, D. Sangaa, V.L. Aksenov, Kinetics of cluster growth in polar solutions of fullerene: experimental and theoretical study of C_{60}/NMP solution. J. Mol. Liq. **175**, 4–11 (2012). https://doi.org/10.1016/j.molliq.2012.08.003
31. N. Jargalan, T.V. Tropin, M.V. Avdeev, V.L. Aksenov, Investigation and modeling of evolution of C_{60}/NMP solution UV-Vis spectra. Nanosyst. Phys. Chem. Math. **7**, 99–103 (2016). https://doi.org/10.17586/2220-8054-2016-7-1-99-103
32. M. Baibarac, L. Mihut, N. Preda, I. Baltog, J.Y. Mevellec, S. Lefrant, Surface-enhanced Raman scattering studies on C_{60} fullerene self-assemblies. Carbon N. Y. **43**, 1–9 (2005). https://doi.org/10.1016/j.carbon.2004.08.020
33. A. Mrzel, A. Mertelj, A. Omerzu, M. Čopič, D. Mihailovic, Investigation of encapsulation and solvatochromism of fullerenes in binary solvent mixtures. J. Phys. Chem. B. **103**, 11256–11260 (1999). https://doi.org/10.1021/jp992637e
34. V.L. Aksenov, Study of fullerene aggregates in pyridine/water solutions, in *AIP Conference Proceedings, AIP*, pp. 66–69 (2001). https://doi.org/10.1063/1.1426823
35. V.L.L. Aksenov, M.V. Avdeev, T.V. Tropin, V.B. Priezzhev, J.W.P. Schmelzer, Model description of aggregation in fullerene solutions, in *AIP Conference Proceedings, AIP*, pp. 37–40 (2005). https://doi.org/10.1063/1.2103816
36. V.L. Aksenov, T.V. Tropin, M.V. Avdeev, V.B. Priezzhev, J.W.P. Schmelzer, Kinetics of cluster growth in fullerene molecular solutions. Phys. Part. Nucl. **36** (2005)
37. V.V. Slezov, J.W.P. Schmelzer, Comments on nucleation theory. J. Phys. Chem. Solids **59**, 1507–1519 (1998). https://doi.org/10.1016/S0022-3697(98)00079-1
38. V.V. Slezov, J. Schmelzer, Kinetics of formation and growth of a new phase with a definite stoichiometric composition. J. Phys. Chem. Solids **55**, 243–251 (1994). https://doi.org/10.1016/0022-3697(94)90139-2
39. V.V. Slezov, Y.J. Tkatch, J. Schmelzer, The kinetics of decomposition of solid solutions. J. Mater. Sci. **32**, 3739–3747 (1997)
40. R. Becker, W. Döring, Kinetische Behandlung der Keimbildung in übersättigten Dämpfen. Ann. Phys. **416**, 719–752 (1935). https://doi.org/10.1002/andp.19354160806

41. N.O. Mchedlov-Petrossyan, N.N. Kamneva, Y.T.M. Al-Shuuchi, A.I. Marynin, S.V. Shekhovtsov, The peculiar behavior of fullerene C_{60} in mixtures of 'good' and polar solvents: colloidal particles in the toluene–methanol mixtures and some other systems. Colloids Surf. A Physicochem. Eng. Asp. **509**, 631–637 (2016). https://doi.org/10.1016/j.colsurfa.2016.09.045
42. M. Alfè, B. Apicella, R. Barbella, A. Bruno, A. Ciajolo, Aggregation and interactions of C_{60} and C_{70} fullerenes in neat N-methylpyrrolidinone and in N-methylpyrrolidinone/toluene mixtures. Chem. Phys. Lett. **405**, 193–197 (2005). https://doi.org/10.1016/j.cplett.2005.02.030
43. M. Alfè, R. Barbella, A. Bruno, P. Minutolo, A. Ciajolo, Solution behaviour of C_{60} fullerene in N-Methylpyrrolidinone/toluene mixtures. Carbon N. Y. **43**, 665–667 (2005). https://doi.org/10.1016/j.carbon.2004.10.017
44. V.L. Aksenov, M.V. Avdeev, T.V. Tropin, M.V. Korobov, N.V. Kozhemyakina, N.V. Avramenko, L. Rosta, Formation of fullerene clusters in the system C_{60}/NMP/water by SANS. Phys. B Condens. Matter. **385–386**, 795–797 (2006). https://doi.org/10.1016/j.physb.2006.06.086
45. O.A. Kyzyma, M.V. Korobov, M.V. Avdeev, V.M. Garamus, S.V. Snegir, V.I. Petrenko, V.L. Aksenov, L.A. Bulavin, Aggregate development in C_{60}/N-methyl-2-pyrrolidone solution and its mixture with water as revealed by extraction and mass spectroscopy. Chem. Phys. Lett. **493**, 103–106 (2010). https://doi.org/10.1016/j.cplett.2010.04.076
46. T.V Tropin, T.O. Kyrey, O.A. Kyzyma, A.V. Feoktistov, M.V. Avdeev, L.A. Bulavin, L. Rosta, V.L. Aksenov, Experimental investigation of C_{60}/NMP/toluene solutions by UV-Vis spectroscopy and small angle neutron scattering. J. Surf. Investig. X-Ray, Synchrotron Neutron Tech. **7**, 5–8 (2013). https://doi.org/10.1134/s1027451013010199
47. O.A. Kyzyma, T.O. Kyrey, M.V. Avdeev, M.V. Korobov, L.A. Bulavin, V.L. Aksenov, Non-reversible solvatochromism in N-methyl-2-pyrrolidone/toluene mixed solutions of fullerene C_{60}. Chem. Phys. Lett. **556**, 178–181 (2013). https://doi.org/10.1016/j.cplett.2012.11.040
48. A.A. Kaznacheevskaya, O.A. Kizima, L.A. Bulavin, A. V. Tomchuk, V.M. Garamus, M.V. Avdeev, Reorganization of the cluster state in a C_{60}/N-Methylpyrrolidone/water solution: Comparative characteristics of dynamic light scattering and small-angle neutron scattering data. J. Surf. Investig. X-Ray, Synchrotron Neutron Tech. **7**, 1133–1136 (2013). https://doi.org/10.1134/s102745101306030x
49. A.D. Bokare, A. Patnaik, Evidence for C_{60} aggregation from solvent effects in [Ps–C_{60}] molecular complex formation. Carbon N. Y. **41**, 2643–2651 (2003). https://doi.org/10.1016/S0008-6223(03)00384-1
50. T.O. Kyrey, O.A. Kyzyma, M.V. Avdeev, T.V. Tropin, M.V. Korobov, V.L. Aksenov, L.A. Bulavin, Absorption characteristics of fullerene C_{60} in N-Methyl-2-Pirrolidone/Toluene mixture, fullerenes. Nanotub. Carbon Nanostruct. **20**, 341–344 (2012). https://doi.org/10.1080/1536383X.2012.655173
51. G.V. Andrievsky, V.K. Klochkov, A.B. Bordyuh, G.I. Dovbeshko, Comparative analysis of two aqueous-colloidal solutions of C_{60} fullerene with help of FTIR reflectance and UV–Vis spectroscopy. Chem. Phys. Lett. **364**, 8–17 (2002). https://doi.org/10.1016/S0009-2614(02)01305-2
52. N. Jargalan, T.V.V. Tropin, M.V.V. Avdeev, V.L.L. Aksenov, Investigation of the dissolution kinetics of fullerene C_{60} in solvents with different polarities by UV-Vis spectroscopy, J. Surf. Investig. X-Ray, Synchrotron Neutron Tech. **9,** 12–16 (2015). https://doi.org/10.1134/s102745101501019x
53. R.S. Ruoff, D.S. Tse, R. Malhotra, D.C. Lorents, Solubility of fullerene (C_{60}) in a variety of solvents. J. Phys. Chem. **97**, 3379–3383 (1993). https://doi.org/10.1021/j100115a049
54. A.A.A.A. Noyes, W.R.W.I. Whitney, The rate of solution of solid substances in their own solutions, J. Am. Chem. Soc. **19**, 930–934 (1897). https://doi.org/10.1021/ja02086a003
55. A. Naumenko, M. Biliy, V. Gubanov, A. Navozenko, Spectroscopic studies of fullerene clusters in N-methyl-2-pyrrolidone, J. Mol. Liq. 1–4 (2017). https://doi.org/10.1016/j.molliq.2017.01.035
56. O.B. Karpenko, V.V. Trachevskij, O.V. Filonenko, V.V. Lobanov, M.V. Avdeev, T.V. Tropin, O.A. Kyzyma, S.V. Snegir, Nmr study of non-equilibrium state of fullerene C_{60} in N-methyl-2-pyrrolidone. Ukr. J. Phys. **57**, 860–863 (2012)

57. J.W.P. Schmelzer, G. Ropke, V.B. Priezzhev, *Nucleation Theory and Applications*, in ed. by J.W.P. Schmelzer, G. Ropke, V.B. Priezzhev (JINR Publishing House, Dubna, 1999), pp. 1–525
58. V.V. Slezov, V.V. Sagalovich, Diffusive decomposition of solid solutions. Sov. Phys. Uspekhi. **30**, 23–45 (1987). https://doi.org/10.1070/PU1987v030n01ABEH002792
59. V.L.L. Aksenov, T.V.V. Tropin, M.V.V. Avdeev, V.B.B. Priezzhev, J.W.P.W.P. Schmelzer, Kinetics of cluster growth in fullerene molecular solutions. Phys. Part. Nucl. **36**, S52–S61 (2005)
60. T.V. Tropin, V.B. Priezzhev, M.V. Avdeev, J.W.P. Schmelzer, V.L. Aksenov, Fullerene cluster formation in carbon disulfide and toluene, fullerenes. Nanotub. Carbon Nanostruct. **14**, 481–488 (2006). https://doi.org/10.1080/15363830600666365
61. V.V. Slezov, J. Schmelzer, J. Möller, Ostwald ripening in porous materials. J. Cryst. Growth **132**, 419–426 (1993). https://doi.org/10.1016/0022-0248(93)90067-7
62. J. Schmelzer, J. Möller, V.V. Slezov, Ostwald ripening in porous materials: The case of arbitrary pore size distributions. J. Phys. Chem. Solids **56**, 1013–1022 (1995). https://doi.org/10.1016/0022-3697(95)00021-6
63. I.S. Gutzow, J.W.P. Schmelzer, *The Vitreous State: Thermodynamics, Structure, Rheology, and Crystallization* (1995)
64. F.M. Kuni, A.I. Rusanov, A.K. Shchekin, A.P. Grinin, Kinetics of aggregation in micellar solutions. Russ. J. Phys. Chem. A **79**, 833–853 (2005)
65. A.P. Grinin, D.S. Grebenkov, Study of relaxation in micellar solution by the numerical experiment. Colloid J. **65**, 552–561 (2003). https://doi.org/10.1023/A:1026111504241
66. T.V. Tropin, M.V. Avdeev, O.A. Kyzyma, V.L. Aksenov, Nucleation theory models for describing kinetics of cluster growth in C_{60}/NMP solutions. Phys. Status Solidi. **247**, 3022–3025 (2010). https://doi.org/10.1002/pssb.201000119
67. T.V. Tropin, M.V. Avdeev, O.A. Kyzyma, R.A. Yeremin, N. Jargalan, M.V. Korobov, V.L. Aksenov, Towards description of kinetics of dissolution and cluster growth in C_{60}/NMP solutions. Phys. Status Solidi. **248**, 2728–2731 (2011). https://doi.org/10.1002/pssb.201100099
68. T.V. Tropin, M.V. Avdeev, V.L. Aksenov, Modeling of the evolution of the cluster-size distribution functions in polar fullerene C_{60} solutions, J. Surf. Investig. X-Ray, Synchrotron Neutron Tech. **3** (2019). https://doi.org/10.1134/S102745101901035X
69. I.M. Lifshits, V.V. Slezov, Kinetics of the diffusion decomposition of supersaturated solid solutions. Zhurnal Eksp. i Teor. Fiz. **35**, 479–492 (1958)
70. A.L. Smith, E. Walter, M.V. Korobov, O.L. Gurvich, Some enthalpies of solution of C_{60} and C_{70}. Thermodynamics of the temperature dependence of fullerene solubility. J. Phys. Chem. **100,** 6775–6780 (1996). https://doi.org/10.1021/jp952873z
71. T.V. Tropin, N. Jargalan, M. V. Avdeev, O.A. Kyzyma, D. Sangaa, V.L. Aksenov, Calculation of the cluster size distribution functions and small-angle neutron scattering data for C_{60}/N-methylpyrrolidone. Phys. Solid State. **56,** 148–151 (2014). https://doi.org/10.1134/s1063783414010363
72. R. Pascova, I. Gutzow, J. Schmelzer, A model investigation of the process of phase formation in photochromic glasses. J. Mater. Sci. **25**, 921–931 (1990). https://doi.org/10.1007/BF03372180
73. V.L. Aksenov, T.V. Tropin, O.A. Kyzyma, M.V. Avdeev, M.V. Korobov, L. Rosta, Formation of C_{60} fullerene clusters in nitrogen-containing solvents. Phys. Solid State **52**, 1059–1062 (2010). https://doi.org/10.1134/S1063783410050367
74. T.V. Tropin, V.L. Aksenov, Theoretical investigation of the cluster size decrease effect on dilution of a solution by water. J. Exp. Theor. Phys. **128**, 274–280 (2019). https://doi.org/10.1134/S1063776119010187
75. P. Jain, S.H. Yalkowsky, Solubilization of poorly soluble compounds using 2-pyrrolidone. Int. J. Pharm. **342**, 1–5 (2007). https://doi.org/10.1016/j.ijpharm.2007.03.056
76. R. Sanghvi, R. Narazaki, S.G. Machatha, S.H. Yalkowsky, Solubility improvement of drugs using N-methyl pyrrolidone. Am. Assos. Pharm. Sci. **9**, 366–376 (2008). https://doi.org/10.1208/s12249-008-9050-z
77. V.L. Aksenov, M.V. Avdeev, T.V. Tropin, V.B. Priezzhev, J.W.P. Schmelzer, Model description of aggregation in fullerene solutions, in *AIP Conference Proceedings, AIP*, pp. 37–40 (2005). https://doi.org/10.1063/1.2103816

78. J. Bartels, U. Lembke, R. Pascova, J. Schmelzer, I. Gutzow, Evolution of cluster size distribution in nucleation and growth processes. J. Non. Cryst. Solids **136**, 181–197 (1991). https://doi.org/10.1016/0022-3093(91)90489-S
79. O.A. Kyzyma, L.A. Bulavin, V.L. Aksenov, T.V. Tropin, M.V. Avdeev, M.V. Korobov, S.V. Snegir, L. Rosta, Aggregation in C 60/NMP, C 60/NMP/water and C 60/NMP/toluene mixtures, fullerenes. Nanotub. Carbon Nanostruc. **16**, 610–615 (2008). https://doi.org/10.1080/15363830802312982